Published in final edited form as:
Science. 2013 November 15; 342(6160): 856–860. doi:10.1126/science.1243147.

Cytoplasmic Volume Modulates Spindle Size During Embryogenesis

Matthew C. Good[1,2,3], **Michael D. Vahey**[2], **Arunan Skandarajah**[2], **Daniel A. Fletcher**[2,4,*], and **Rebecca Heald**[1,*]

[1]Department of Molecular and Cellular Biology, University of California, Berkeley

[2]Department of Bioengineering and Biophysics Group, University of California, Berkeley

[3]Miller Institute for Basic Research in Science, University of California, Berkeley

[4]Physical Biosciences Division, Lawrence Berkeley National Laboratory, Berkeley CA, 94720, USA

Abstract

Rapid and reductive cell divisions during embryogenesis require that intracellular structures adapt to a wide range of cell sizes. The mitotic spindle presents a central example of this flexibility, scaling with the dimensions of the cell to mediate accurate chromosome segregation. To determine whether spindle size regulation is achieved through a developmental program or is intrinsically specified by cell size or shape, we developed a system to encapsulate cytoplasm from *Xenopus* eggs and embryos inside cell-like compartments of defined sizes. Spindle size was observed to shrink with decreasing compartment size, similar to what occurs during early embryogenesis, and this scaling trend depended on compartment volume rather than shape. Thus, the amount of cytoplasmic material provides a mechanism for regulating the size of intracellular structures.

While mechanisms that set eukaryotic cell size by coordinating growth and division rates have been uncovered (1-3), much less is known about how the size and shape of a cell affect its physiology. Recent work has suggested mechanisms by which cell boundaries or size can control biochemical reactions (2), constrain cytoskeletal assembly (4-6), and dictate the positioning of internal structures (7, 8). The size-scaling problem is most acute during early embryo development when cell size changes rapidly. For example, over the first 10 hours of amphibian embryogenesis cell diameter may decrease 100-fold – from a 1.2 mm egg to 12 μm diameter blastomeres – due to cell division in the absence of growth (9). How micron-scale organelles and cellular structures adapt and function across a wide spectrum of cell sizes is an emerging area of research (10-14).

*To whom correspondence should be addressed, bheald@berkeley.edu, fletch@berkeley.edu.

The authors declare no competing financial interests.

Data described can be found in the main figures and online supplement.

Supporting Online Materials: Includes Materials and methods, Supplemental text, Supplemental figures S1 – S11 and References (32 – 39).

Here we focused on the mitotic spindle, a dynamic bipolar structure consisting of microtubules and many associated factors that must be appropriately sized to accurately distribute chromosomes to daughter cells. During development, spindle size correlates with cell size in the embryos of invertebrates (15, 16), amphibians (9) (fig. S1), and mammals (17). However, it is unknown whether spindle size is governed by compositional changes as part of a developmental blueprint, or if spindle size is coupled directly to physical properties of the cell, such as size and shape. Although molecular mechanisms of spindle size regulation have been proposed (9-13), the existence of a causal relationship between cell size and spindle size remains unclear.

Due to the difficulty of modulating cell size in vivo, we investigated spindle size scaling by developing an in vitro system of cell-like droplets of varying size containing *Xenopus* egg or embryo cytoplasm. *Xenopus* egg extracts transit the cell cycle in the absence of cell boundaries and recapitulate many cell biological activities in vitro, including spindle assembly (18, 19). To match cell size changes during *Xenopus* embryogenesis, we tuned compartment volume 1,000,000-fold using microfluidic systems (4, 5) (Fig. 1A, and fig. S2). A polyethylene glycol (PEG)-ylated stearate served as a surfactant to prevent droplets from coalescing and to prevent cytoplasmic proteins from interacting with the boundary (Fig.1A).

Metaphase spindle length and width scaled with droplet size in vitro (Fig.1, B and C, and fig. S3). Spindles, which normally have a steady-state length of 35-40 μm in bulk egg extract (20), became smaller as the size of the encapsulating droplet decreased (Fig. 1C and fig. S3). Spindle size-scaling was approximately linear in droplet diameters ranging from 20 – 80 μm (Fig. 1C), whereas in larger droplets, spindle size matched that of unencapsulated egg extracts. Spindle assembly efficiency decreased in very small droplets and dropped to zero in droplets with a diameter less than 20 μm (fig. S3C and D). Thus, two regimes of scaling were observed: one in which spindle size was coupled to droplet diameter and a second in which they were uncoupled. These two regimes were similar to spindle scaling trends observed in vivo during early *Xenopus* embryogenesis (Fig. 1C and D, Fig. S1B) (9). Thus, compartmentalization is sufficient to recapitulate spindle size scaling during embryogenesis in the absence of any developmental cues (e.g. transcription).

We considered two possible explanations for the scaling of spindle size with cell or droplet size. The position of cell or droplet boundaries could directly influence spindle size through interaction with microtubules. Alternatively, cytoplasmic volume could limit the amount of material for assembly, which has been proposed for centrosome size regulation in *C. elegans* (12, 21) and spindle size regulation in mouse and sea snail embryos (17, 22). To distinguish between these two possibilities we compared spindle size scaling in droplets that were spherical or compressed into a disk-like shape (z-height ∼ 25 μm) (fig. S4B). Spindle length and assembly efficiency in different shaped droplets collapsed onto the same curve when plotted against volume but not diameter, suggesting that spindle assembly is dependent on amount of cytoplasm rather than the position of the compartment boundaries (Fig.2 and fig. S4C). While spindles were positioned near the center of cells in the embryo, they appeared more randomly distributed when formed in droplets (fig. S4D) (31). Although the cell boundary plays a crucial role in positioning and could affect spindle size in vivo, we did not

observe an effect in droplets (fig. S4D). Thus compartment volume, not boundary interactions dictate spindle size in our system.

To elucidate how spindle size scales with compartment volume we considered a limiting component mechanism, in which the amount of particular molecules per cell regulates spindle assembly. While multiple components could become limiting, we focused our attention on tubulin, the subunit of microtubules and the major structural component of the spindle whose levels have been implicated in regulating spindle size (23). Because cellular tubulin concentration and the number and length of microtubules in the egg extract spindle have been characterized (24, 25), it was possible to determine what fraction of soluble tubulin within a given volume remained in the cytoplasm after spindle assembly. We used this information to create a simplified quantitative model that predicted spindle size based on compartment volume (Fig. 3A and fig. S5). The model assumes an available pool of soluble α/β-tubulin dimers, which is depleted as the spindle assembles, and depends on both cytoplasmic volume and spindle volume. Because tubulin concentration is known to affect microtubule dynamics (26, 27), we hypothesized that this depletion might drive volume-dependent spindle scaling. Combining this idea with measured spindle parameters (24, 25) and the observation that tubulin density in the spindle does not change with spindle size (fig. S6) (28), we derived an analytical model for volume-dependent spindle scaling that agrees quantitatively with our data both in droplets (Fig. 3B and fig. S5C) and in cells during embryogenesis (fig. S5D) (31).

A key prediction of this model is that the soluble tubulin concentration after spindle assembly should be lower for smaller cells. We measured the fluorescence intensity of tubulin in the cytoplasm and spindle as a function of cell volume (fig. S6A) and found that cytoplasmic tubulin was significantly depleted in cells smaller than 150 μm in diameter, with up to 60% of the total cellular tubulin incorporated into the spindle in the smallest cells (Fig. 3C and fig. S6B). This result is quantitatively consistent with our model (Fig. 3C) and rules out other models in which the spindle assembles from a constant fraction of cellular material. While our analysis suggests that tubulin is necessary to maintain spindle size, it is likely not to be sufficient. The addition of tubulin to egg extracts did not alter spindle scaling in droplets (fig. S7), presumably because the levels of other spindle assembly factors were also limiting. In summary, although the model described here is general and can be applied to other molecular components that are enriched in the spindle, its quantitative agreement with measured data suggests that tubulin depletion plays an important role in volume-dependent spindle scaling.

Volume offers a useful mechanism for directly modulating spindle size throughout development. Because cell size varies within an embryo, and even within individual stages of development (fig S8A), scaling mechanisms based only on developmental timing or cytoplasmic composition would not couple spindle size to cell size, potentially leading to spindle positioning errors. We found that spindle length and cell volume correlated across most stages of *X. laevis* early embryogenesis (Fig. 4A), and also within individual developmental stages (fig. S8B and C), in support of volume-dependent scaling in vivo. To demonstrate that cytoplasmic volume regulates spindle size independent of developmental stage, we encapsulated Stage 4 (8 cell) and Stage 8 (~4000 cell) embryo extracts. In the

largest droplets, maximum spindle size was consistent with results in unencapsulated extracts (29), and depended on developmental stage (Fig. 4B). Nonetheless, encapsulated mitotic spindles from both extracts exhibited volume-dependent scaling (Fig. 4B), showing that cytoplasmic volume and composition together control spindle size during *X. laevis* embryogenesis.

To determine whether cytoplasmic volume-dependent spindle scaling is conserved in other organisms, we encapsulated egg extracts from a related frog species, *Xenopus tropicalis*, which generate smaller spindles than *X. laevis* extracts, in part due to higher microtubule severing activity of p60 Katanin (20, 30). Like *X. laevis* spindles, *X. tropicalis* spindles scaled with compartment volume, both in vitro (fig. S9, A and B) and in vivo (Fig. 4A and fig. S10B). Combined with recent data for spindle size in embryos of the mammal *M. musculus* (17), these findings indicate conservation of volume-dependent scaling in vertebrate evolution. Although the upper limits to spindle size vary in embryonic cells among these organisms (fig. S10C), large portions of the scaling curves closely overlapped (fig. S10D).

Taken together, these results suggest that volume-dependent spindle size scaling is conserved across spindle architectures (meiotic and mitotic), developmental stages, and vertebrate species. Previous reports on spindle scaling factors have focused primarily on compositional differences between cells or cytoplasmic extracts. We have identified cell volume as a physicochemical scaling mechanism that regulates spindle size through limiting amounts of cytoplasmic material, acting in concert with other mechanisms that alter activity of microtubule regulatory factors (25, 28-30). Altogether, mechanisms altering the concentration or activity of cytoplasmic scaling factors appear to modulate maximum and minimum spindle size, whereas cytoplasmic volume couples spindle size to cell size (fig. S11). We propose that the amounts of certain molecules known to be important for spindle assembly, including but not limited to tubulin, are responsible for this coupling, which weakens as cell volume increases and the components required for assembly are no longer limiting.

Supplementary Material

Refer to Web version on PubMed Central for supplementary material.

Acknowledgments

This work was supported by fellowships from the Miller Institute for Basic Science Research (M.C.G.), National Institutes of Health (M.D.V.), and National Science Foundation (A.S.). This work was also supported by NIH grants (GM074751) (D.A.F.) and (GM098766) (R.H.). We thank J. Wilbur, K. Helmke, F. Nedelec, K. Weis, M. Welch, H. Ramage, K. Nyberg, N. Metrakos, the Berkeley BioChIP NSF REU program, and members of the Heald and Fletcher labs.

References

1. Kafri R, et al. Dynamics extracted from fixed cells reveal feedback linking cell growth to cell cycle. Nature. 2013; 494:480–483. [PubMed: 23446419]
2. Turner JJ, Ewald JC, Skotheim JM. Cell size control in yeast. Curr Biol. 2012; 22:R350–359. [PubMed: 22575477]

3. Tzur A, Kafri R, LeBleu VS, Lahav G, Kirschner MW. Cell growth and size homeostasis in proliferating animal cells. Science. 2009; 325:167–171. [PubMed: 19589995]
4. Pinot M, et al. Effects of confinement on the self-organization of microtubules and motors. Curr Biol. 2009; 19:954–960. [PubMed: 19427215]
5. Pinot M, et al. Confinement induces actin flow in a meiotic cytoplasm. Proc Natl Acad Sci U S A. 2012; 109:11705–11710. [PubMed: 22753521]
6. Laan L, et al. Cortical dynein controls microtubule dynamics to generate pulling forces that position microtubule asters. Cell. 2012; 148:502–514. [PubMed: 22304918]
7. Minc N, Burgess D, Chang F. Influence of cell geometry on division-plane positioning. Cell. 2011; 144:414–426. [PubMed: 21295701]
8. OM L, et al. Mitotic rounding alters cell geometry to ensure efficient bipolar spindle formation. Dev Cell. 2013:270–283. [PubMed: 23623611]
9. Wuhr M, et al. Evidence for an upper limit to mitotic spindle length. Curr Biol. 2008; 18:1256–1261. [PubMed: 18718761]
10. Chan YH, Marshall WF. How cells know the size of their organelles. Science. 2012; 337:1186–1189. [PubMed: 22955827]
11. Dumont S, Mitchison TJ. Force and length in the mitotic spindle. Curr Biol. 2009; 19:R749–761. [PubMed: 19906577]
12. Goehring NW, Hyman AA. Organelle growth control through limiting pools of cytoplasmic components. Curr Biol. 2012; 22:R330–339. [PubMed: 22575475]
13. Goshima G, Scholey JM. Control of mitotic spindle length. Annu Rev Cell Dev Biol. 2010; 26:21–57. [PubMed: 20604709]
14. Levy DL, Heald R. Mechanisms of intracellular scaling. Annu Rev Cell Dev Biol. 2012; 28:113–135. [PubMed: 22804576]
15. Greenan G, et al. Centrosome size sets mitotic spindle length in Caenorhabditis elegans embryos. Curr Biol. 2010; 20:353–358. [PubMed: 20137951]
16. Hara Y, Kimura A. An Allometric Relationship between Mitotic Spindle Width, Spindle Length, and Ploidy in Caenorhabditis elegans Embryos. Mol Biol Cell. 2013
17. Courtois A, Schuh M, Ellenberg J, Hiiragi T. The transition from meiotic to mitotic spindle assembly is gradual during early mammalian development. J Cell Biol. 2012; 198:357–370. [PubMed: 22851319]
18. Desai A, Murray A, Mitchison TJ, Walczak CE. Chapter 20 The Use of Xenopus Egg Extracts to Study Mitotic Spindle Assembly and Function in Vitro. 1998; 61:385–412.
19. Hannak E, Heald R. Investigating mitotic spindle assembly and function in vitro using Xenopus laevis egg extracts. Nat Protoc. 2006; 1:2305–2314. [PubMed: 17406472]
20. Brown KS, et al. Xenopus tropicalis egg extracts provide insight into scaling of the mitotic spindle. J Cell Biol. 2007; 176:765–770. [PubMed: 17339377]
21. Decker M, et al. Limiting amounts of centrosome material set centrosome size in C. elegans embryos. Curr Biol. 2011; 21:1259–1267. [PubMed: 21802300]
22. Conklin EG. Cell size and nuclear size. Journal of Experimental Zoology. 1912; 12:1–98.
23. Lattao R, Bonaccorsi S, Gatti M. Giant meiotic spindles in males from Drosophila species with giant sperm tails. J Cell Sci. 2012; 125:584–588. [PubMed: 22389398]
24. Brugues J, Nuzzo V, Mazur E, Needleman DJ. Nucleation and transport organize microtubules in metaphase spindles. Cell. 2012; 149:554–564. [PubMed: 22541427]
25. Loughlin R, Heald R, Nedelec F. A computational model predicts Xenopus meiotic spindle organization. J Cell Biol. 2010; 191:1239–1249. [PubMed: 21173114]
26. Brun L, Rupp B, Ward JJ, Nedelec F. A theory of microtubule catastrophes and their regulation. Proc Natl Acad Sci U S A. 2009; 106:21173–21178. [PubMed: 19948965]
27. Janson ME, de Dood ME, Dogterom M. Dynamic instability of microtubules is regulated by force. J Cell Biol. 2003; 161:1029–1034. [PubMed: 12821641]
28. Reber SB, et al. XMAP215 activity sets spindle length by controlling the total mass of spindle microtubules. Nat Cell Biol. 2013; 15:1116–1122. [PubMed: 23974040]

29. Wilbur JD, Heald R. Mitotic spindle scaling during Xenopus development by kif2a and importin alpha. Elife. 2013; 2:e00290. [PubMed: 23425906]
30. Loughlin R, Wilbur JD, McNally FJ, Nedelec FJ, Heald R. Katanin contributes to interspecies spindle length scaling in Xenopus. Cell. 2011; 147:1397–1407. [PubMed: 22153081]
31. A description of the spindle centering analysis and a detailed derivation of the limiting component model can be found in the supplementary materials.
32. Khokha MK, et al. Techniques and probes for the study of Xenopus tropicalis development. Dev Dyn. 2002; 225:499–510. [PubMed: 12454926]
33. McDonald JC, et al. Fabrication of microfluidic systems in poly (dimethylsiloxane). Electrophoresis. 2000; 21:27–40. [PubMed: 10634468]
34. Preibisch S, Saalfeld S, Tomancak P. Globally optimal stitching of tiled 3D microscopic image acquisitions. Bioinformatics. 2009; 25:1463–1465. [PubMed: 19346324]
35. Sive, HL.; Grainger, RM.; Harland, RM. Early development of Xenopus laevis : a laboratory manual. Cold Spring Harbor Laboratory Press; Cold Spring Harbor, N.Y.: 2000. p. ixp. 338
36. Showell C, Conlon FL. Natural mating and tadpole husbandry in the western clawed frog Xenopus tropicalis. Cold Spring Harb Protoc. 2009; 2009 pdb prot5292.
37. Becker BE, Gard DL. Visualization of the cytoskeleton in Xenopus oocytes and eggs by confocal immunofluorescence microscopy. Methods Mol Biol. 2006; 322:69–86. [PubMed: 16739717]
38. Gard DL, Kirschner MW. Microtubule assembly in cytoplasmic extracts of Xenopus oocytes and eggs. J Cell Biol. 1987; 105:2191–2201. [PubMed: 3680377]
39. Dinarina A, et al. Chromatin shapes the mitotic spindle. Cell. 2009; 138:502–513. [PubMed: 19665972]

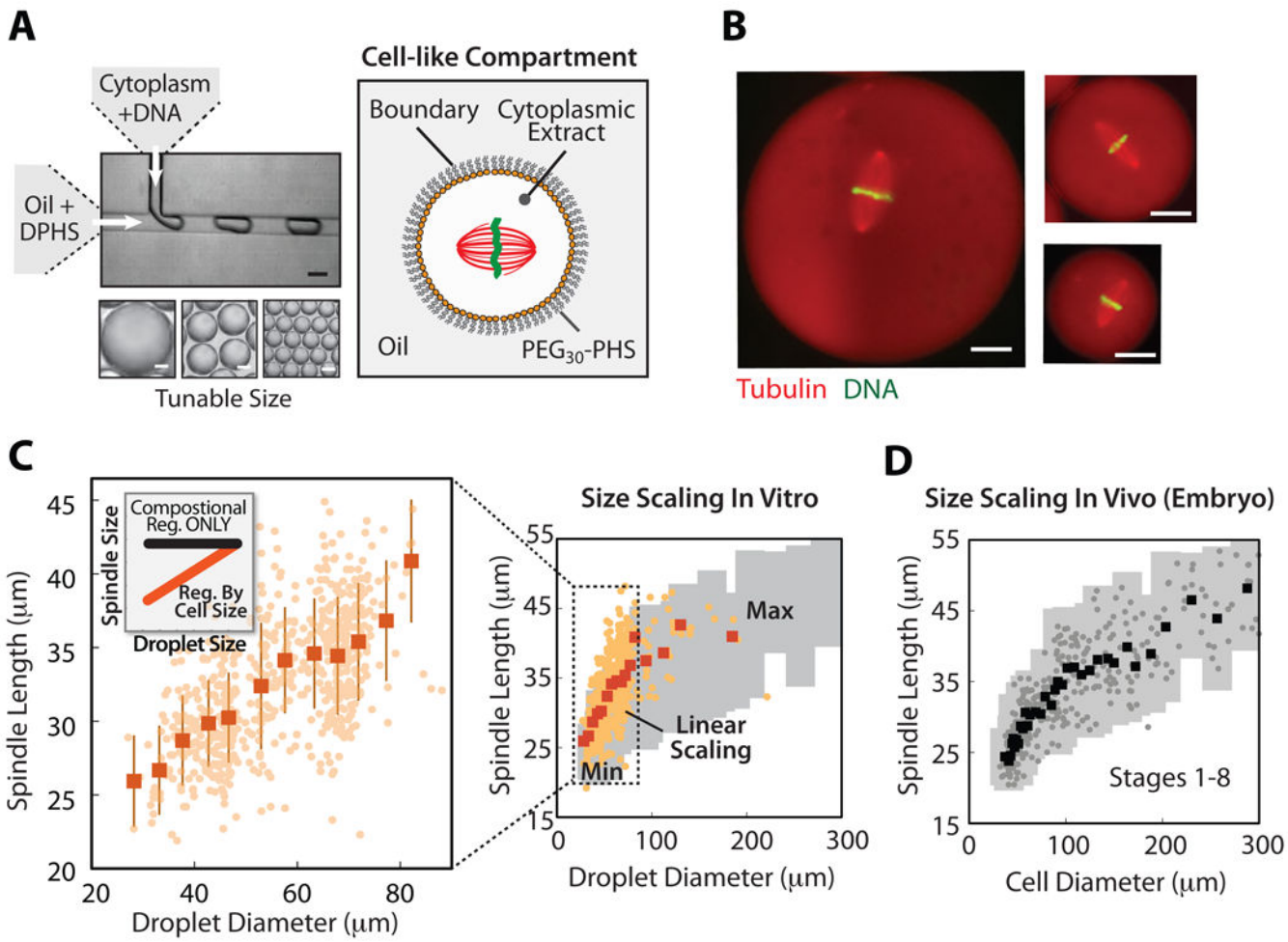

Figure 1. Spindle Length Scales with Compartment Size In Vitro and In Vivo

(A) System for creating cell-like compartments in vitro, including a passivated boundary, cell-free cytoplasm capable of assembling metaphase spindles (*Xenopus* egg or embryo extracts), and tunable compartment size. (B) Spindles in droplets – compressed to improve image quality - corresponding to spheres 80, 55, and 40 μm in diameter. Uneven shading is due to image stitching. (C) Spindle length in encapsulated *X. laevis* egg extract scaled with droplet size in vitro. *Left*: Linear scaling regime. *Inset*: scaling prediction. Raw data (orange circles), and average spindle length (orange squares) +/- SD across 5 μm intervals in droplet diameter are shown. P-value ($< 10^{-60}$) and R^2 (0.34) calculated from linear fit to raw droplet data in 20-80 μm diameter range. *Right*: full scaling curve in vitro. For comparison, gray bars indicate two standard deviations from average embryo data in D. (D) Spindle length scaling in vitro mirrored length scaling in the *X. laevis* embryo through Stage 8 with similar linear scaling regimes and a plateau where spindle size was uncoupled from compartment size. Raw data from embryos across 5 μm intervals in cell diameter (gray circles), and average spindle length (black squares) +/- 2 SD (thick error bars) are shown. Scale bar 20 μm.

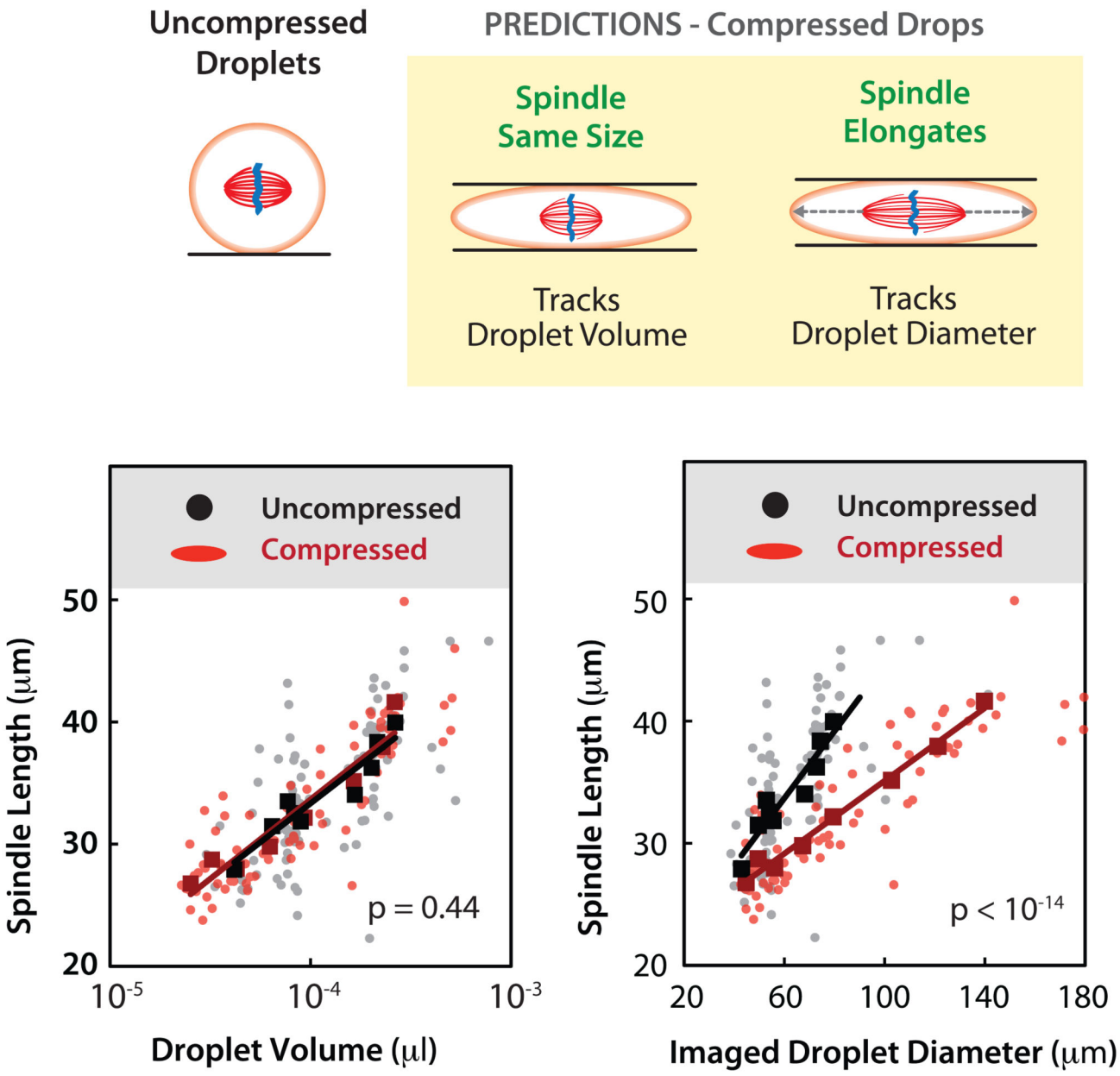

Figure 2. Cytoplasmic Volume Sets Spindle Size In Vitro

To distinguish between boundary- and volume-sensing models, spindle length scaling was compared in uncompressed (spherical) and compressed (disk-like) droplets (details in fig. S4B). Spindle length scaling in both droplet geometries appeared identical when plotted as a function of droplet volume, supporting a volume-sensing mechanism. Spindle scaling curves did not overlay when plotted as a function of projected (imaged) droplet diameter, ruling out boundary-sensing. Raw data points (circles: gray = uncompressed, red = compressed) and spindle length, averaged across ten droplets (squares: black = uncompressed, red = compressed), are shown. Raw data was fit to a log function in volume plot and linear function in diameter plot (black line, $R^2 = 0.45$ (uncompressed), and red line, $R^2 = 0.79$

(compressed)). P-values indicate statistical difference between y-intercepts of compressed vs. uncompressed regression lines, calculated using an analysis of covariance.

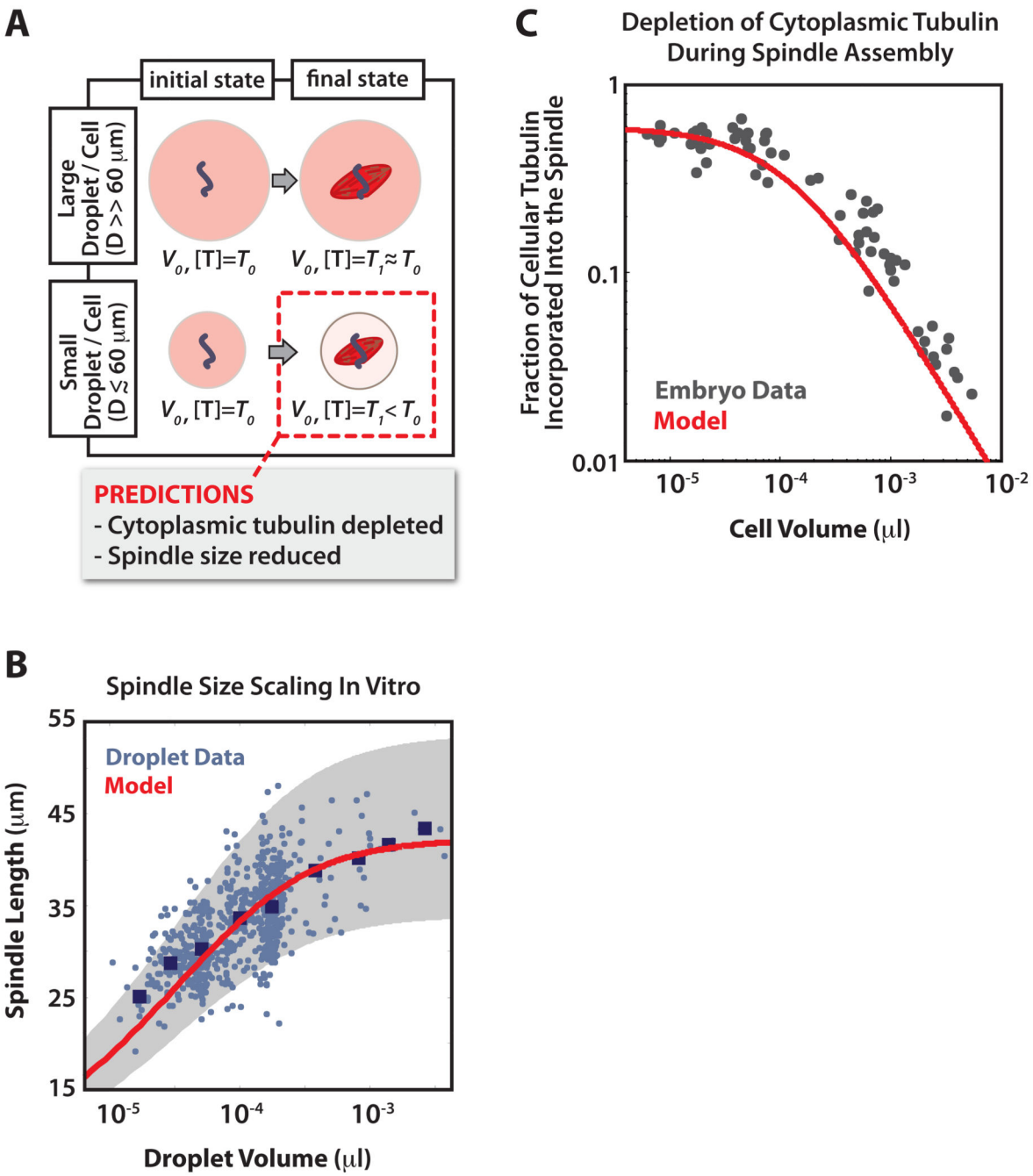

Figure 3. A Limiting Component Model for Spindle Size Regulation

(A) Schematic of limiting component model (for more details, see fig. S5A and supplemental text). (B) Limiting tubulin model accurately predicted *X. Laevis* spindle length from droplet volume in vitro. Raw data from droplets (blue circles) and binned averages (dark blue squares) was compared to the model. Shaded gray regions represent model predictions across a range of parameter values (fig. S5B); the red line shows the prediction for intermediate values. (C) Cytoplasmic tubulin became significantly depleted as cell size decreased during *X. laevis* embryogenesis. Comparison of model prediction (red) and

experimental data (gray) for the fraction of total cellular tubulin incorporated in the spindle as a function of cell volume. Model used parameter values that gave best agreement in fig. S5C and D.

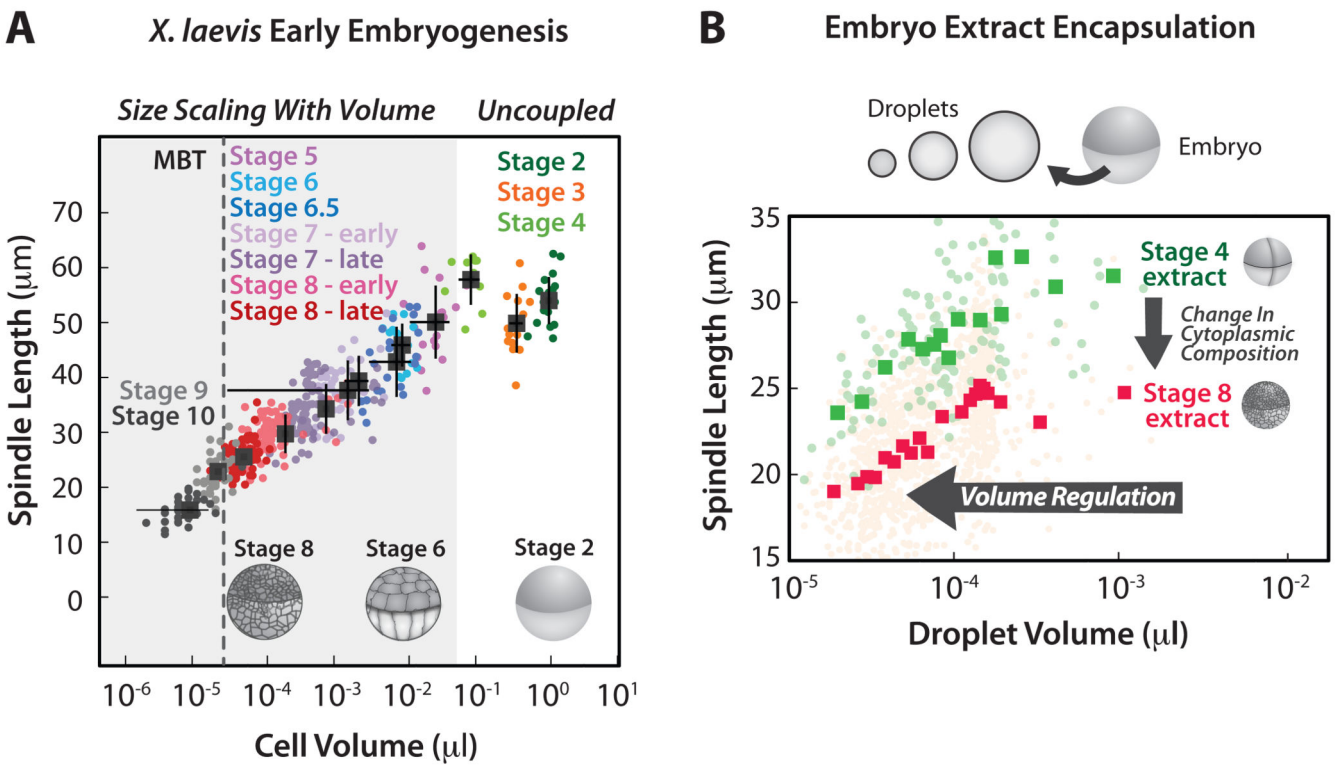

Figure 4. Cell Volume and Composition Control Spindle Size During *Xenopus* Early Embryogenesis

(A) Spindle length scaled linearly with cell volume across a broad range of developmental stages during early *X. laevis* embryogenesis (Stages 5-10). Spindle length had an upper limit and was uncoupled from cell volume in Stages 2-4. Raw data (colored circles) and stage-averaged cell diameter and spindle length (black squares) +/- SD are shown. (B) Despite having distinct maximum spindle lengths, coupled to developmental stage (Stage 4 = green, Stage 8 = red), the length of *X. laevis* embryo extract mitotic spindles scaled with compartment volume in vitro. This result suggested that changes in cytoplasmic volume and composition work in concert to regulate spindle size. Raw data points (light circles) and bin-averaged spindle length (squares) were calculated for 5 μm intervals in droplet diameter across the 20-80 μm range of droplet diameters (wider interval were used for averaging in largest droplets because data was sparse).